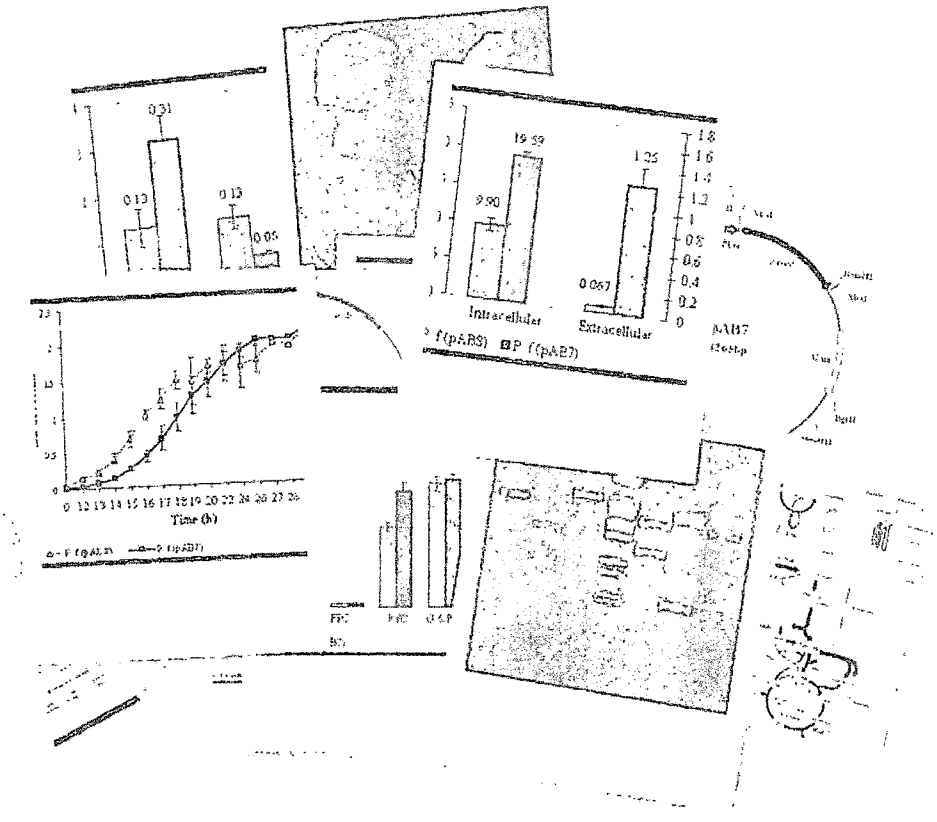

CHAPTER 5

Effect of constitutive heterologous overexpression of *E. coli* citrate synthase (*cs*) gene on glucose metabolism of *P. fluorescens* ATCC 13525

"Research is to see what everybody else has seen and to think what nobody else has thought"

- Albert Szent-Gyorgyi

5.1: INTRODUCTION

Citrate synthase (CS) is a ubiquitous enzyme that catalyzes the first committed step of Tricarboxylic acid (TCA) cycle involving condensation of oxaloacetate (OAA) and acetyl-CoA to form citrate. Hence it is the key enzyme governing the carbon flux into the TCA cycle which plays a dual function in the production of cellular energy and biosynthetic precursors under aerobic conditions and only latter under anaerobic conditions. CS is a non-redundant enzyme indispensable in the carbon metabolism under aerobic as well as anaerobic conditions (Park et al., 1994). However, in organisms like *Bacillus subtilis* and *E. coli* (Patton et al., 1993; Jin and Sonenshein, 1994) two *cs* genes are localized in the chromosome while in *Rhizobium tropici*, of the two *cs* genes one is chromosomally localized and another is found in the symbiotic plasmid (Hernández-Lucas et al., 1995). Similarly, two isozymes of CS, CSI and CSII, have also been demonstrated in *Pseudomonas aeruginosa* PAC514; however, whether they are encoded by distinct structural genes or not is not known (Solomon and Weitzman, 1983; Mitchell and Weitzman, 1986; Mitchell et al 1995). In *B. subtilis* two CS might have specialized roles under different metabolic conditions with *citZ* gene encoded CS being important for sporulation (Jin and Sonenshein, 1996), in *R. tropici* both CS were required for nodulation while in *P. aeruginosa* PAC514, CSI was found during exponential phase while CSII predominated in stationary phase and both were demonstrated to be integral part of a multienzyme complex of TCA cycle enzymes catalyzing the consecutive reactions from fumarate to 2-oxoglutarate (Mitchell, 1996).

5.1.1: Biochemical basis of citric acid accumulation in fungi, yeast and bacteria

Citric acid is an industrially important metabolic product and hence physiological and biochemical conditions allowing citrate accumulation have been extensively studied and reviewed (Berovic and Legisa, 2007; Legisa and Mattey, 2007; Papagianni, 2007). The bioprocess of citric acid formation was optimized for commercial production using *Aspergillus niger* grown on molasses, sucrose or glucose (Xu et al., 1989; Ali et al., 2002; El-Holi and Al-Delaimy, 2003; Haq et al., 2004) and alternatively *Candida* strains (including *Yarrowia lipolytica*) utilizing various carbon sources including n-alkanes, glucose, raw glycerol, ethanol and galactose (Anastassiadis and Rehm, 2005; Rymowicz et al., 2006). Microbial citric acid production and secretion are distinct yet interdependent processes and its biochemical basis is not very clear.

Citric acid overflow in *A. niger* requires a unique combination of nutrient conditions, i.e. excessive concentrations of carbon source, hydrogen ions and dissolved oxygen or suboptimal concentrations of certain trace metals and phosphate, which synergistically influence the yield of citric acid (Mlakar and Legisa, 2006). Glycolytic flux in *A. niger* is chiefly regulated by phosphofructokinase-1 (PFK-1), which is susceptible to activation by fructose-2,6-bisphosphate (F-2,6-bP), AMP and NH_4^+ and inhibition by PEP, citrate and ATP (Rohr, Kubicek and Kominek, 1996). Efficient citric acid accumulation in *A. niger* in presence of excess sugar is attributed to increased intracellular levels of F-2,6-bP which relieves the ATP inhibition of PFK-1 leading to increased and uncontrolled glycolytic rate, which is prerequisite for citric acid accumulation (Kubicek-Pranz et al., 1990; Mlakar and Legisa, 2006).

NH_4^+ levels regulate citrate overproduction in *A. niger* but the relationship between NH_4^+ levels in the medium and its uptake in correlation with glucose transport is unclear (Papagianni et al., 2005). During the early phase of citric acid fermentation by *A. niger* on glucose, uptaken NH_4^+ combines with glucose to form glucosamine. Glucosamine-6-phosphate deaminase has been suggested to be responsible for glucosamine accumulation as a consequence of direct competition with PFK-1 for the common substrate fructose-6-phosphate (F-6-P). Glucosamine accumulation appears to reduce the glycolytic flux by removal of the key intermediate subsequently leading to slower citrate accumulation rate (Solar et al., 2008). When NH_4^+ is depleted from the medium, one of the substrates for glucosamine deaminase becomes limiting and hence F-6-P can be catabolized by PFK-1 leading to enhanced glycolytic flux.

Citric acid production process in yeast required nitrogen depletion in the fermentation medium, increase in intracellular NH_4^+ concentration, induction of specific active citrate transport system for citrate secretion and was further enhanced by media optimization such as iron depletion (Anastassiadis and Rehm, 2005). Apart from fungi and yeast, several mutants of coryneform bacteria like *Corynebacterium*, *Arthrobacter* and *Brevibacterium* produce citric acid from n-paraffin and related substrates (Rohr, Kubicek and Kominek, 1996). Many other bacteria mainly including *Bacillus* sp., *Bradyrhizobium* strain and *Citrobacter koseri* are known to secrete low levels of citric acid but the biochemical basis of its formation is not well understood (Carson et al., 1992; Gyaneshwar et al., 1998; Khan et al., 2006).

5.1.2: Genetic manipulations for citric acid overproduction

Mathematical modeling of citric acid production in *A. niger* predicted that increase in the glucose influx could increase the citric acid productivity by 45% (Guebel and Torres Darias, 2001). Additionally, increase in the mitochondrial phosphate carrier activity was predicted to enhance citric acid production in *A. niger*. However, overexpression of *pfk,* pyruvate kinase (*pk*) and citrate synthase (*cs*) genes in *A. niger* were not successful in increasing the citrate production (Ruijter et al. 1997; 2000). On the other hand, isocitrate lyase (*icl*) gene overexpression in *Yarrowia lipolytica* shifted the citrate/isocitrate ratio towards citric acid formation on glycerol, glucose and sucrose (Forster et al., 2007a). Recombinant *Y. lipolytica* expressing invertase and *icl* genes produced high yields of citric acid from sucrose, with a concomitant reduction in the formation of the by-product, isocitrate (Forster et al., 2007b). Amongst bacteria, *E. coli* K and B isocitrate dehydrogenase (*icd*) mutants accumulated high levels of citrate when grown on glucose with a concomitant increase in CS activity upto more than 2 fold (Lakshmi and Helling, 1976; Aoshima et al., 2003). Similarly, *B. subtilis icd* mutant in early stationary phase accumulated ~15 fold higher intracellular citrate levels as compared to the wild type (Matsuno et al., 1999).

Collectively, metabolic studies on citric acid producing fungi, yeasts and *E. coli* demonstrated that high citric acid yields could be attained on glucose and depending on the host metabolism; glucose transport, flux though catabolic pathways and the regulatory mechanisms influenced by intracellular metabolite pools appear to facilitate the citrate accumulation. However, role of CS in citrate accumulation is unclear.

5.1.3: Effects of *cs* gene overexpression in *E. coli* and other microorganisms

Despite the key position of CS, less information is available regarding the effects of *cs* gene manipulations on cellular metabolism and their role in citric acid overproduction. *E. coli* lacking functional *cs* gene failed to utilize glucose unless supplemented with glutamate (or other TCA cycle intermediates) and had reduced growth as compared to the wild type (Gruer et al., 1997; Vandedrinck et al., 2001; De Maeseneire et al., 2006). On the other hand, *cs* gene overexpression or underexpression in *E. coli* had no effect on growth on glucose while on acetate as sole carbon source; CS levels strongly affected the growth rate (Walsh and Koshland, 1985a; Vandedrinck et al., 2001). *glt*A gene overexpression in *E. coli* increased the maximum cell dry weight by

23% and reduced acetate secretion (De Maeseneire et al., 2006). Overexpression of *cs* gene in *A. niger* did not alter citric acid production (Guebel and Torres Darias, 2001).

Overexpression of mitochondrial citrate synthase in *Arabidopsis thaliana* improved growth on a phosphorus-limited soil and also could improve the growth of carrot cells on Al-phosphate medium; the effect suspected to be due to enhanced secretion of citric acid (Koyama et al., 1999; 2000). *P. aeruginosa cs* gene overexpression in tobacco (*Nicotiana tabacum*; CSb lines) was suggested to improve P-uptake and Al tolerance *via* citrate efflux (de la Fuente et al., 1997; López-Bucio et al., 2000) but this strategy was not reproducible for citric acid mediated enhancement in P uptake and Al-tolerance (Delhaize et al., 2001). On the other hand, overexpression of mitochondrial *cs* gene in *S. cerevisiae* and canola (*Brassica napus cv Westar*) enhanced the Al-tolerance due to increased citrate accumulation (Anoop et al, 2003).

5.1.4: Rationale for *cs* gene overexpression in pseudomonads

Glucose metabolism in *Aspergillus* spp., *E. coli* and *Bacillus* respectively, occurs via traditional EMP pathway whereas pseudomonads utilize glucose by two different routes; periplasmic direct oxidation pathway mediated by PQQ-GDH and intracellular phosphorylative oxidation which ultimately follow the ED pathway (Lessie and Phibbs, 1984). In addition, glucose flux through TCA cycle in pseudomonads is high resulting in lower acetate overflow (Fuhrer et al., 2005). Many pseudomonads possess pyruvate carboxylase (PYC) as well as phosphoenolpyruvate carboxylase (PPC) involved at the anaplerotic node. Unlike *E. coli*, pseudomonads possess a citrate transporter which would facilitate the growth on citric acid (Stover et al., 2000; Nelson et al., 2002).

E. coli CS is type II, typical of gram-negative bacteria functioning as a homo-hexamer with monomer size of ~48kDa and is allosterically inhibited by NADH and α-ketoglutarate (Danson et al., 1979; Park et al., 1994; Nguyen et al., 2001). *P. aeruginosa cs* gene has been cloned, sequenced and is demonstrated to be allosterically inhibited by NADH (Donald et al., 1989). Citrate overproduction by pseudomonads would not only be industrially relevant, but could also promote plant growth by facilitating the acquisition of P and Fe from soils (López-Bucio et al., 2000; Guerinot et al., 1990). The present work describes the effect of *E. coli cs* gene overexpression on glucose metabolism and its role in altering the citrate levels in *Pseudomonas fluorescens* 13525.

5.2: EXPERIMENTAL DESIGN

5.2.1: Bacterial strains used in this study

Strains	Relevant characteristics	Reference
E. coli JM101	Host strain for routine DNA manipulation experiments and plasmid maintenance	Sambrook and Russell, 2001
E. coli W620	*cs* mutant strain exhibiting glutamate auxotrophy, used for functional analysis of pAB7 and pAB9 plasmids carrying *E. coli cs* gene; Str^r	*E. coli* Genetic Stock Center
P. fluorescens ATCC 13525	Wild Type strain	MTCC, Chandigarh
Pf(pAB8)	*P. fluorescens* 13525 with pAB8; Km^r	This study
Pf(pAB7)	*P. fluorescens* 13525 with pAB7; Km^r	This study
Pf(pAB9)	*P. fluorescens* 13525 with pAB9; Km^r	This study
Pf(pBBR1MCS-2)	*P. fluorescens* 13525 with pBBR1MCS-2; Km^r	This study

Table 5.1: List of bacterial strains used. Detailed characteristics of these strains and plasmids are given in Section 2.1. Parent strains and the transformants of *E. coli* and *Pseudomonas* were respectively grown at 37°C and 30°C with streptomycin and kanamycin as and when required, at final concentrations varying for rich and minimal media as described in Section 2.2.

5.2.2: Construction of pAB7 and pAB9 containing *E. coli cs* gene under *lac* promoter

Incorporation of *E. coli cs* in pUCPM18

E. coli cs gene was obtained as 1,312bp DNA fragment by digesting pCS-Ec plasmid (4,237bp) with SacI and BamHI enzymes. The hence obtained fragment was gel eluted, purified and ligated to purified SacI-BamHI digested pUCPM18 plasmid (5,349bp). The resultant pAB6 plasmid (6,646bp) containing inserted *cs* gene in correct orientation with respect to *lac* promoter of pUCPM18 was identified by restriction pattern. Subsequently, kanamycin resistance gene (*km^r*) was incorporated in pAB6 in order to procure appropriate selection marker for *Pseudomonas* transformants. The requisite *km^r* gene was obtained as a purified 1,637bp DNA fragment by digesting pYanni3 plasmid (7,535bp) with XhoI-HindIII and was ligated to SalI-HindIII digested

pAB6 to yield pAB7 (8,265bp). The desired plasmid was selected as kanamycin resistant colonies on Luria Agar and was confirmed by restriction digestion pattern of the isolated plasmid. The pAB7 plasmid was separately digested with XbaI to release 1,294bp *cs* gene fragment and the remaining plasmid backbone was self-ligated to obtain pAB8 (6,971bp) containing only km^r gene in pUCPM18 which was used as the control plasmid for all experiments.

Incorporation of *E. coli cs* in pBBR1MCS-2

pAB7 plasmid described above contained *E. coli cs* gene under *lac* promoter of pUCPM18 which is a pRO1614 replicon based plasmid (West et al., 1994; Farinha and Kropinski, 1990). In order to consider the influence of plasmid copy number in the present metabolic engineering studies, the same *E. coli cs* gene was also cloned under the *lac* promoter of another broad-host-range pBBR1MCS-2 plasmid having pBBR1 origin of replication which is different from that in pUCPM18 (Kovach et al, 1995; Section 2.1). Use of pBBR1MCS-2 for expression studies is also reported for *P. putida* KT2442 (Pérez-Pantoja et al., 2000).

A 1,294bp DNA fragment containing *E. coli cs* gene obtained by digesting pAB7 plasmid (described above) with XbaI was purified and ligated to purified XbaI digested pBBR1MCS-2 plasmid to obtain pAB9 plasmid (6,438bp). The ligation mixture was transformed into *E. coli* JM101 and the transformants were obtained based on blue-white selection on agar plates containing kanamycin and X-Gal. The plasmids isolated from white colonies were subjected to restriction digestion using XbaI, EcoRI and BamHI to screen the clone containing *E. coli cs gene* in correct orientation with respect to *lac* promoter. All the molecular biology techniques like plasmid DNA isolation and transformation, restriction digestion, gel elution, ligation and gel electrophoresis were performed as in Section 2.4.

5.2.3: Functional confirmation of CS expressed from pAB7 and pAB9

E. coli W620, which exhibited glutamate auxotrophy due to mutation in *cs* gene, was used to determine the functionality of the *cs* gene in pAB7 and pAB9. pAB7 and pAB9 along with the respective controls pAB8 and pBBR1MCS-2 plasmids were transformed into *E. coli* W620 (**Table 5.1**, Section 2.4.2). The transformants on agar plates with streptomycin and kanamycin (doses as recommended in Section 2.2)

confirmed the presence of respective plasmids. Subsequently these were subjected to auxotrophy complementation studies (Section 2.8).

5.2.4: Development of *P. fluorescens* 13525 harboring *E. coli cs* gene

The recombinant plasmids pAB7, pAB8, pAB9 and pBBR1MCS-2 were transformed in *P. fluorescens* 13525 (Section 2.4.2). The transformants were selected on kanamycin selection plates and were confirmed by fluorescence (Section 2.3).

5.2.5: Effect of *E. coli cs* gene expression on the physiology and glucose metabolism of *P. fluorescens* 13525

P. fluorescens transformants were subjected physiological experiments involving growth and organic acid production profiles on M9 minimal medium with 100mM glucose as carbon source. The samples withdrawn at regular interval were analyzed for $O.D._{600nm}$, pH, and extracellular glucose (Section 2.9). Stationary phase culture harvested at the time of pH drop was subjected organic acid estimation (Section 2.9.3; 2.11). The physiological parameters were calculated as in section 2.9.3. The enzyme assays were performed as described in Section 2.10, with PPC, PYC, G-6-PDH and GDH being assayed in mid-log to late-log phase cultures while CS, ICL and ICDH being assayed in the stationary phase cells.

5.3: RESULTS

5.3.1: Construction of *Pseudomonas* stable plasmid containing *E. coli cs* gene under *lac* promoter

Based on the above strategies, pAB7 plasmid containing *E. coli cs* gene under *lac* promoter of pUCPM18 plasmid with km^r gene, along with the vector control pAB8 containing only km^r gene in pUCPM18, were constructed. Alternatively, pAB9 containing *cs* gene under *lac* promoter of pBBR1MCS-2 inherently containing km^r gene, was also constructed. The schematic representation of the cloning procedures discussed in Section 5.2.2 is depicted in **Fig. 5.1.** All plasmids were confirmed based on restriction digestion pattern (**Fig. 5.2 a, b, c and d**). These were subjected to confirmatory experiments to demonstrate the expression of a functional CS. Estimated copy numbers of pAB7 and pAB9 plasmids in *P. fluorescens* 13525 were 14±2 and 29±5 respectively.

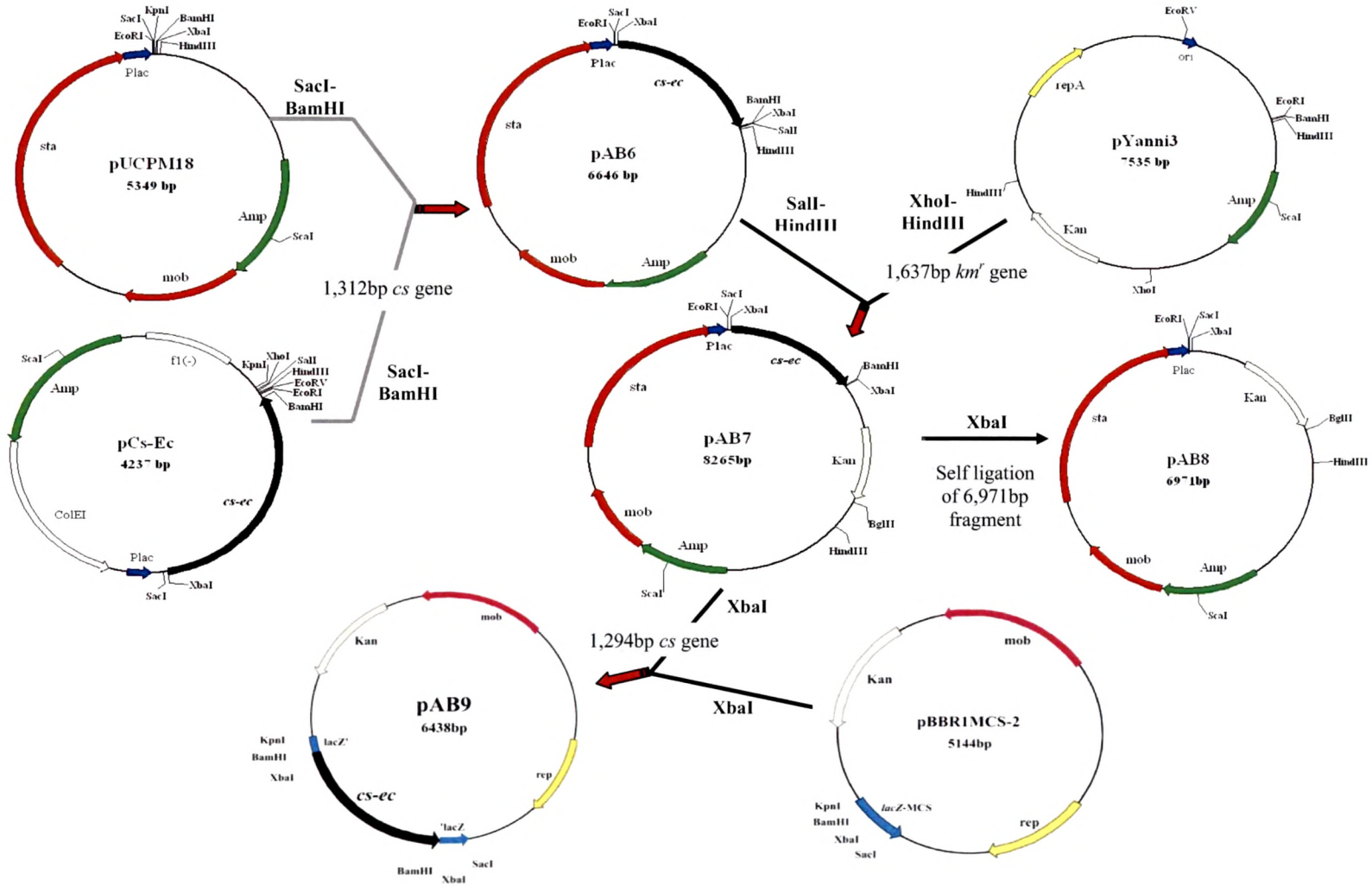

Fig. 5.1: Schematic representation of construction of pseudomonad stable vectors containing *E. coli cs* gene under *lac* promoter

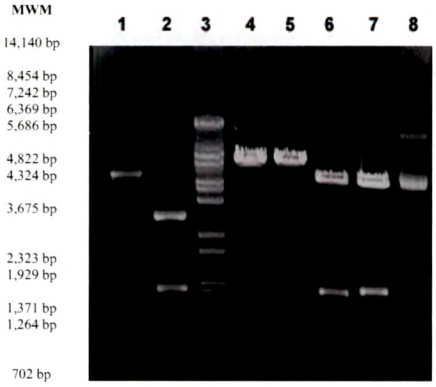

Fig. 5.2a: Restriction digestion pattern for pAB6. Lane 1: pUCPM18 digested with SacI-BamHI (5,334bp, 15bp); Lane 2: pBluscriptIISK(-)Cs-Ec digested with SacI-BamHI (1,312bp, 2,925bp); Lane 3: Molecular Weight Marker (MWM)-Lambda DNA cut with BstEII; Lane 4: pAB6 linearised with SacI (6,646bp); Lane 5: pAB6 linearised with BamHI (6,646bp); Lane 6: pAB6 digested with SacI-BamHI (5,344bp, 1,312bp); Lane 7: pAB6 digested with XbaI (5,352bp, 1,294bp); Lane 8: pAB6 plasmid undigested

Fig. 5.2b: Restriction digestion pattern for pAB7. Lane 1: pAB6 digested with SalI-HindIII (6,628bp, 18bp); Lane 2: pYanni3 digested with XhoI-HindIII (3,742bp, 2,156bp, 1,637bp); Lane 3: pAB7 linearized with BamHI (8,265bp) Lane 4: Molecular Weight Marker (MWM)-Lambda DNA cut with BstEII; Lane 5: pAB7 digested with EcoRI-HindIII (5,298bp, 2,967bp); Lane 6: pAB7 digested with XbaI (6,971bp, 1,294bp); Lane 7: pAB7 digested with XbaI-HindIII (5,328bp, 1,643bp, 1,294bp).

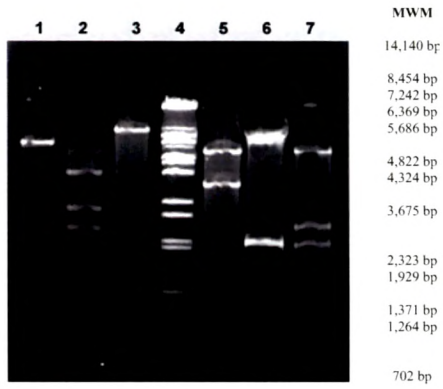

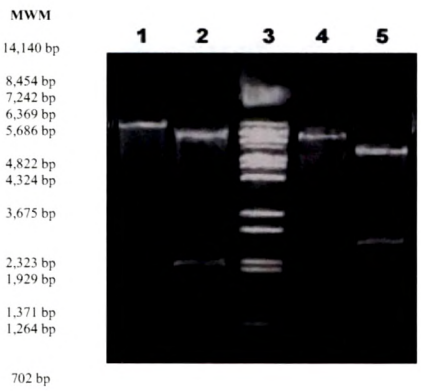

Fig. 5.2c: Restriction digestion pattern for pAB8. Lane 1: pAB7 linearized with BamHI (8,265bp); Lane 2: pAB7 digested with XbaI (1,294bp, 6,971bp); Lane 3: Molecular Weight Marker (MWM)-Lambda DNA cut with BstEII; Lane 4: pAB8 linearised with XbaI (6,971bp); Lane 5: pAB8 digested with EcoRI-HindIII (5,298bp, 1,673bp)

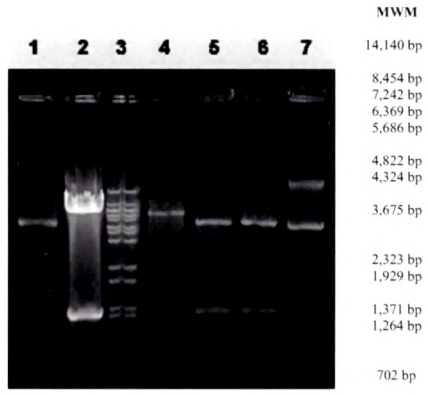

Fig. 5.2d: Restriction digestion pattern for pAB9. Lane 1: pBBR1MCS-2 digested with XbaI (5,144bp); Lane 2: pAB7 digested with XbaI (1,294bp, 6,971bp); Lane 3: Molecular Weight Marker (MWM)-Lambda DNA cut with BstEII; Lane 4: pAB9 linearised with EcoRI (6,438bp); Lane 5: pAB9 digested with XbaI (5,144bp, 1,294bp); Lane 7: pAB9 digested with BamHI (5,138bp, 1,300bp); Lane 8: pAB9 plasmid undigested

5.3.2: *E. coli cs* mutant complementation

E. coli cs mutant strain harboring the pAB7, pAB8, pAB9 and pBBR1MCS-2 plasmids were subjected to growth on M9 minimal medium containing glucose as carbon source in presence and absence of glutamate. *E. coli cs* mutant strain harboring pAB7 and pAB9 could grow on glucose when induced with 0.1mM IPTG without glutamate supplementation unlike the controls pAB8 and pBBR1MCS-2 (**Fig. 5.3**).

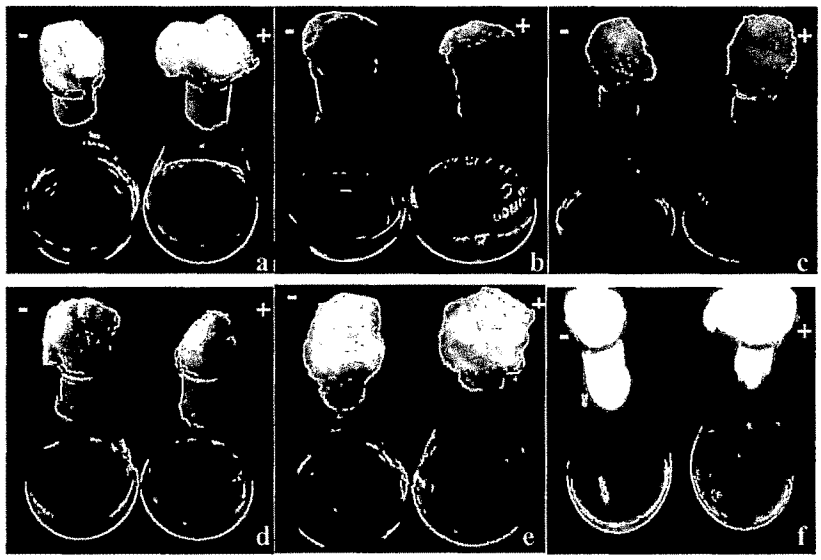

Fig. 5.3: Complementation of *E. coli* W620 mutant phenotype by pAB7 and pAB9 plasmids. **a**: *E. coli* W620-deletion mutant of *cs* gene **b**: *E. coli* W620 with pAB8 plasmid; **c**: *E. coli* W620 with pAB7 plasmid uninduced **d**: *E. coli* W620 with pAB7 plasmid induced with 0.1mM IPTG **e**: *E. coli* W620 with pBBR1MCS-2 plasmid **e**: *E. coli* W620 with pAB9 plasmid induced with 0.1mM IPTG. Growth is monitored on M9 medium with 0.2% glucose (Section 2.8.) –/+ at the corners of each image indicates absence and presence of 340μg/ml glutamate in the medium, respectively.

5.3.3: Heterologous overexpression of *E. coli cs* gene in *P. fluorescens* 13525

P. fluorescens 13525 harboring pAB7 plasmid {*Pf*(pAB7)} had 107.30 ± 9.7U of CS activity in presence of 100mM glucose which was ~2 fold higher than the control *Pf* (pAB8) which had 51.41 ± 3.07U CS activity. On the other hand, *Pf*(pAB9) had 58.07 ± 8.03U which was ~1.6 fold higher than its control *Pf* (pBBR1MCS-2), which showed 36.47 ± 3.62U CS activity.

5.3.4: Effect of *E. coli cs* overexpression on growth, biomass and glucose utilization of *P. fluorescens* 13525

Both *Pf* (pAB7) and the control *Pf* (pAB8) had similar growth profiles on excess glucose and could acidify the extracellular medium within 30h (**Table 5.2; Fig. 5.4**). Glucose consumption in *Pf* (pAB7) reduced by ~1.3 fold as compared to *Pf* (pAB8) while specific growth rate, specific total glucose utilization rate, biomass yield and total amount of glucose utilized after 30h remained unaffected (**Table 5.2**). Similar effect was observed in *Pf* (pAB9) and *Pf* (pBBR1MCS-2) which acidified the extracellular medium within 42h. Glucose consumed in *Pf* (pAB9) reduced by ~1.3 fold as compared to *Pf* (pBBR1MCS-2) with other physiological parameters remaining unaltered.

Amongst the controls *Pf* (pAB8) and *Pf* (pBBR1MCS-2), the specific growth and total glucose utilization rates of the latter were lower by ~2 and 3.5 folds respectively. A concomitant reduction in total glucose utilized and glucose consumption was also observed in *Pf* (pBBR1MCS-2) as compared to *Pf* (pAB8) maintaining the biomass yield.

Bacterial Strain	Sp. growth rate $k\ (h^{-1})^a$	Total glucose utilized (mM)[b]	Glucose consumed (mM)[b]	Biomass yield $Y_{dcw/Glc}$[a] (g/g)	Sp. glucose utilization rate Q_{Glc}[a] ($g.g\ dcw^{-1}.hr^{-1}$)
***Pf* (pAB8)**	0.69 ± 0.04	66.88 ± 3.84	60.02 ± 2.27	0.15 ± 0.02	7.10 ± 0.74
***Pf* (pAB7)**	0.75 ± 0.04 ^{ns}	66.94 ± 2.99 ^{ns}	50.62 ± 1.31**	0.17 ± 0.05 ^{ns}	8.55 ± 1.56 ^{ns}
***Pf* (pBBR1MCS-2)**	0.33 ± 0.03 $^{\alpha}$	52.12 ± 2.96 $^{\beta}$	45.50 ± 2.21 $^{\gamma}$	0.10 ± 0.02 $^{ns'}$	2.63 ± 0.62 $^{\alpha}$
***Pf* (pAB9)**	0.38 ± 0.02 ^{ns}	49.64 ± 1.86 ^{ns}	34.36 ± 2.54*	0.13 ± 0.05 ^{ns}	2.57 ± 0.59 ^{ns}

Table 5.2: Physiological variables and metabolic data from *P. fluorescens cs* transformants grown on M9 medium with 100mM glucose. The results are expressed as Mean ± S.E.M of readings from 6-10 independent observations. [a] Biomass yield $Y_{dcw/Glc}$, specific growth rate (k) and specific glucose consumption rate (Q_{Glc}) were determined from the mid-log phase of each experiment. [b] Total glucose consumed and glucose uptaken were determined at the time of pH drop (30h for *Pf* (pAB7)/*Pf* (pAB8) and 42h for *Pf* (pBBR1MCS-2)/*Pf* (pAB9). *Comparison of parameters with respective controls; α, β, ns' Comparison between parameters of two controls *Pf* (pAB8) and *Pf* (pBBR1MCS-2). $^{\alpha}$ P<0.001; $^{\beta, **}$ P<0.01; $^{\gamma, *}$ P<0.05.

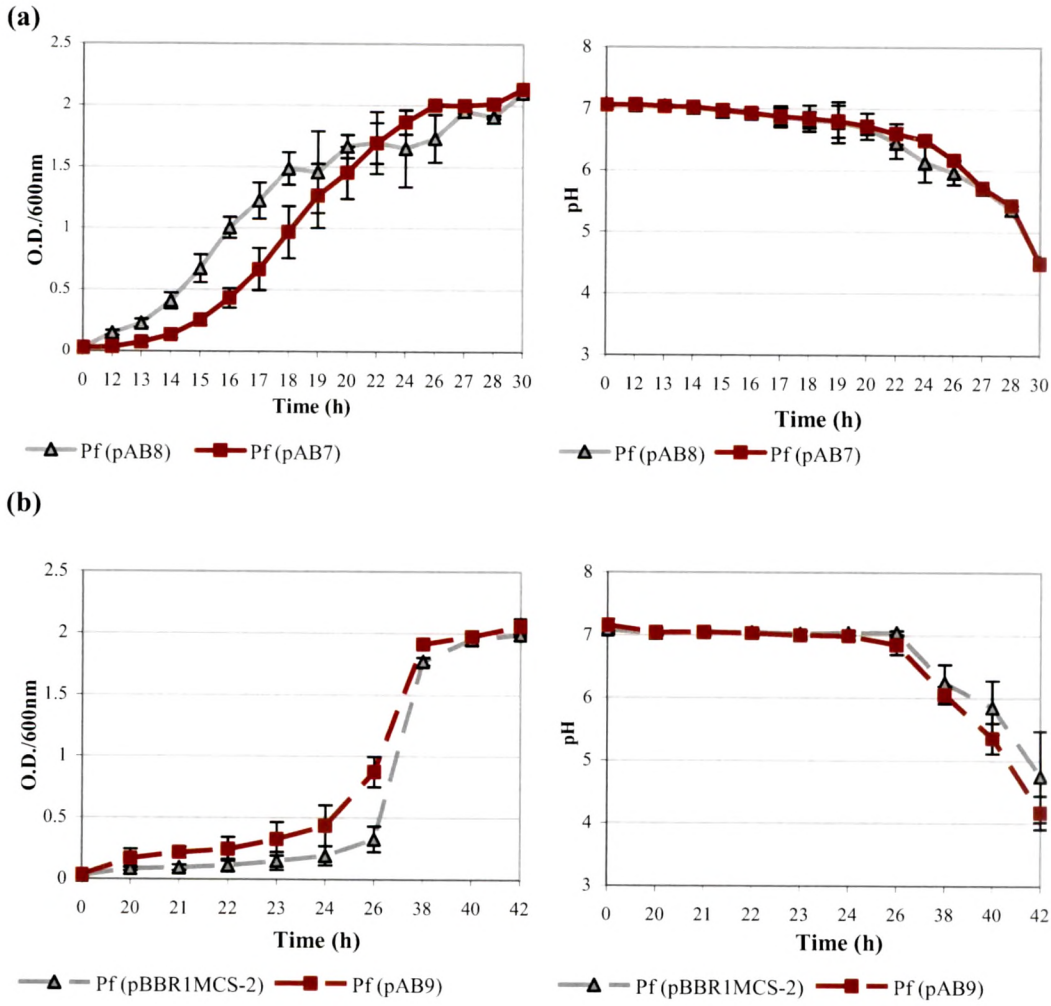

Fig. 5.4 Growth and pH profiles of *P. fluorescens* 13525 *cs* transformants on M9 minimal medium with 100mM glucose. The values plotted represent the Mean±S.D of 6-8 independent observations.

5.3.5: Biochemical effects of *E. coli cs* gene overexpression in *P. fluorescens* 13525

(i) Organic acid secretion

Stationary phase culture supernatants of *Pf* (pAB7), *Pf* (pAB8), *Pf* (pAB9) and *Pf* (pBBR1MCS-2) contained varying amounts of gluconic, pyruvic and acetic acids. At the end of 30h, the extra-cellular culture supernatant of *Pf* (pAB7) contained ~2.7 and ~2.5 fold higher levels and yield ($Y_{G/A}$), respectively, of gluconic acid as compared to the control *Pf* (pAB8) (**Fig. 5.5 a and b**). On the other hand, pyruvic acid levels and yield in

the extracellular medium decreased significantly by about 2.2 and 2.8 fold respectively, while acetic acid yields increased by ~1.8 fold. The *cs* gene overexpression not only caused quantitative changes in secretion of gluconic, pyruvic and acetic acids but also qualitative changes by significantly increasing the citric acid secretion. Interestingly, the citric acid levels and yield in the extracellular medium of *Pf* (pAB7) increased by ~19 and 26 fold, respectively, as compared to the control (**Fig. 5.5 c and d**). Corresponding intracellular citric acid levels and yield were ~2 and 2.3 fold higher in *Pf* (pAB7), respectively.

Similar alterations in organic acid secretion were monitored in *P. fluorescens* 13525 expressing *cs* gene from *lac* promoter of pBBR1MCS-2. Gluconic acid levels and yields in *Pf* (pAB9) increased by ~2.2 fold as compared to the control (**Fig. 5.5 e and f**). Pyruvic acid levels and yields were reduced by ~1.5 fold but acetic acid levels remained unaltered. In contrast to *Pf* (pAB7), no citric acid was secreted in *Pf* (pAB9).

Comparing only the controls, *Pf* (pAB8) and *Pf* (pBBR1MCS-2), similar levels of gluconic, pyruvic and acetic acids were secreted. Citric acid was not at all detected in *Pf* (pBBR1MCS-2) while its levels in *Pf* (pAB8) were very low.

(ii) Alterations in PYC, GDH G-6-PDH, ICDH and ICL activities

Alterations in physiological variables and organic acid profile in response to the targeted *cs* gene overexpression were investigated at the level of key enzymes of glucose catabolism. In *Pf* (pAB7), the periplasmic GDH activity increased by ~1.6 fold while G-6-PDH remained unaltered as compared to control *Pf* (pAB8) (**Fig. 5.6**). Interestingly, PYC activity in *Pf* (pAB7) increased by ~1.4 fold as compared to *Pf* (pAB8). On the other hand, GDH and PYC activities in *Pf* (pAB9) increased by ~2.3 and 1.2 fold respectively, while G-6-PDH remained unaltered. In the stationary phase, ICL and ICDH activities remained unaltered in *Pf* (pAB7) and *Pf* (pAB9) both as compared to their respective control, albeit ICL activity was very low at the glucose concentration used. PPC activity was negligible in all these transformants.

Comparing amongst controls, *Pf* (pAB8) and *Pf* (pBBR1MCS-2), the latter exhibited ~3.8, 1.4, 1.6 and 1.5 fold reduced GDH, PYC, CS and ICDH activities, respectively. However, G-6-PDH activity was similar.

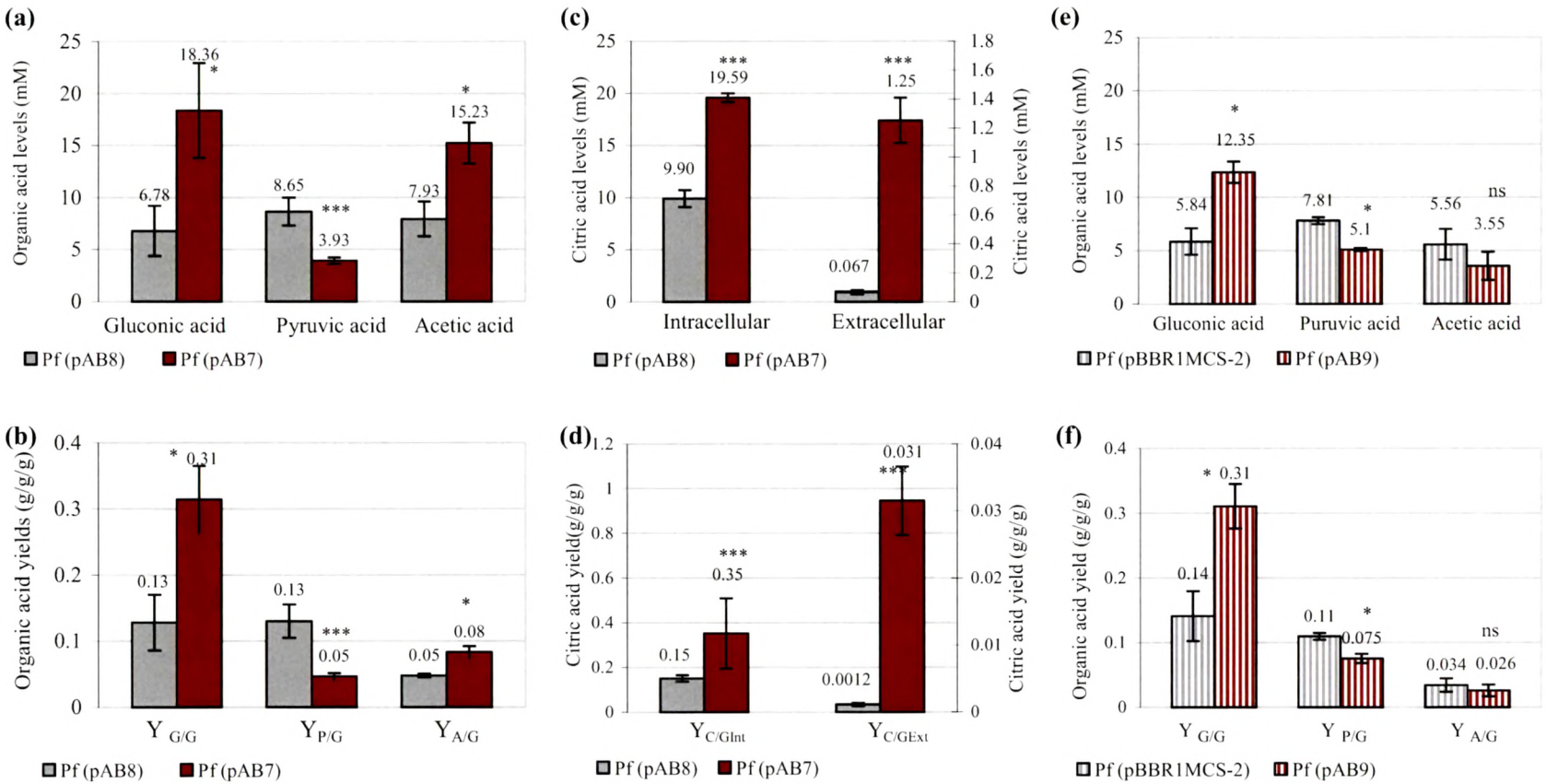

Fig. 5.5: Organic acid production from *P. fluorescens* 13525 *cs* transformants. Gluconic, pyruvic, and acetic acids levels and yields ($Y_{G/G}$, $Y_{P/G}$, and $Y_{A/G}$) in **(a, b)** *Pf* (pAB7), *Pf* (pAB8) and **(e, f)** *Pf* (pAB9), *Pf* (pBBR1MCS-2), respectively. **(c, d)** Citric acids levels and yield ($Y_{C/G\ ext}$ $Y_{C/G\ int}$) in *Pf* (pAB7), *Pf* (pAB8). Organic acid yields were estimated from stationary phase cultures grown on M9 medium with 100mM glucose and are expressed as g/g of glucose utilized/g dry cell mass. Results are expressed as Mean ±S.E.M of 4-7 independent observations. * P<0.05, *** P<0.001, ns=non-significant.

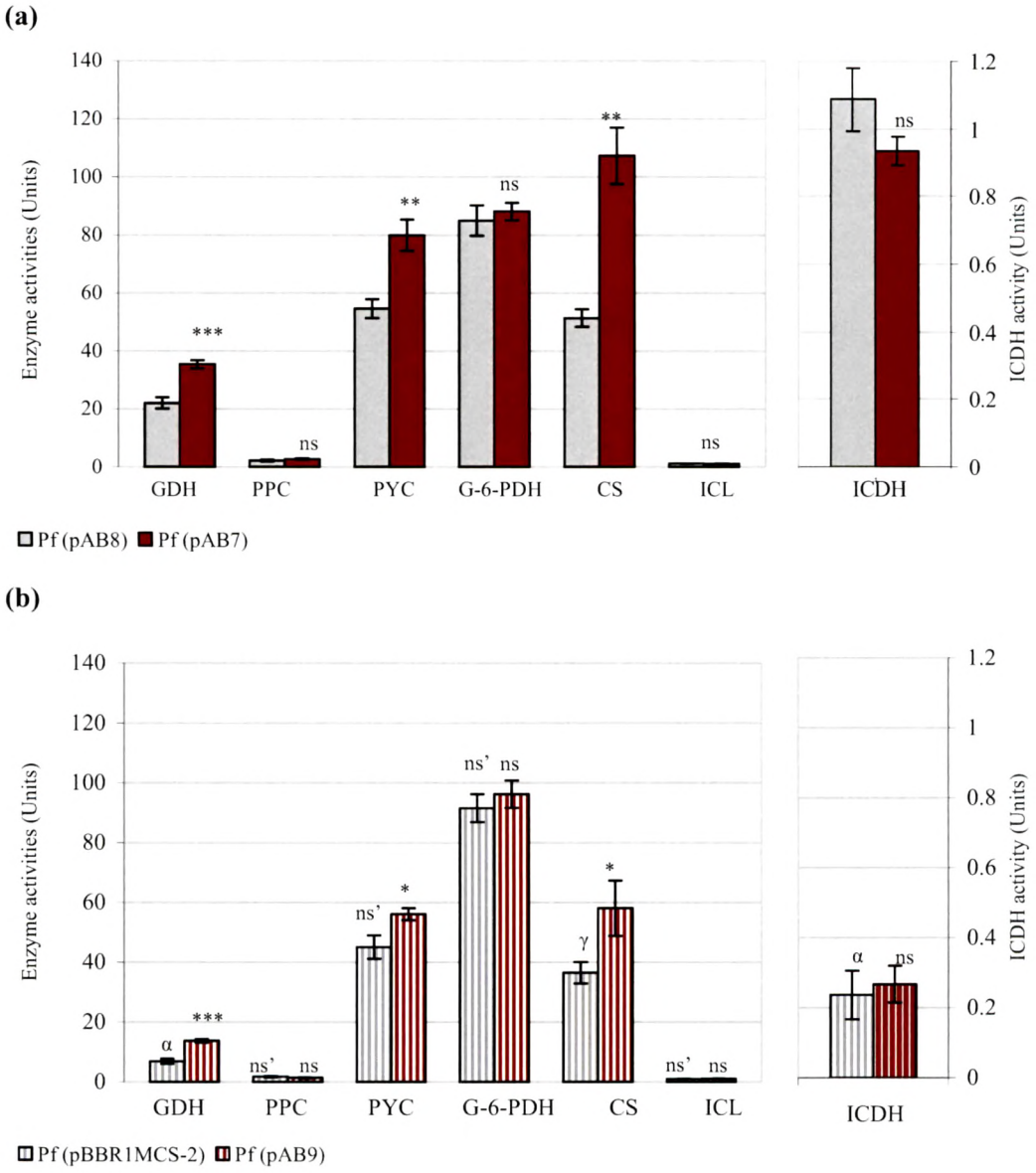

Fig. 5.6: Activities of enzymes PPC, PYC, GDH, G-6-PDH, ICDH and ICL in *P. fluorescens* 13525 *cs* transformants. The activities have been estimated using (**a**) *Pf* (pAB7), *Pf* (pAB8) and (**b**) *Pf* (pAB9), *Pf* (pBBR1MCS-2) cultures grown on M9 minimal medium with 100mM glucose. All the enzyme activities were estimated from mid log phase to late log phase cultures except CS, ICDH and ICL which were estimated in stationary phase. All the enzyme activities are represented in the units of nmoles/min/mg total protein, except ICDH activity which is depicted in the units of µmoles/min/mg total protein. The values are depicted as Mean ± S.E.M of 6-8 independent observations. *Comparison of parameters with respective controls; α, γ Comparison between parameters of two controls *Pf* (pAB8) and *Pf* (pBBR1MCS-2). ***, α P<0.001, **, β P<0.01, *, γ P<0.05, ns= non-significant.

5.4: DISCUSSION

Metabolic studies on citric acid producing fungi, yeasts and *E. coli* K and B *icd* mutants demonstrated that citric acid yields were dependent on the levels of glycolytic as well as TCA cycle enzymes (Alvarez-Vasquez et al., 2000; Aoshima et al., 2003; Anastassiadis and Rehm, 2005; Legisa and Mattey, 2007). Results of the present study demonstrate the effect of overexpression of *E. coli cs* gene in metabolically distinct *P. fluorescens* 13525, schematically represented in **Fig. 5.7**.

E. coli cs gene under *lac* promoter was constitutively expressed upto 2 fold higher in *Pf* (pAB7) which was in accordance with the reports that *lac* promoter is constitutively expressed in pseudomonads (Labes et al., 1990). However, the expression was much less compared to ~12 fold increase demonstrated for *S. elongatus* PCC 6301 *ppc* gene from the same vector in this organism (Chapter 3); the reasons for which are unclear. Interestingly, homologous *cs* gene overexpression from *tac* promoter in *E. coli* increased CS activity upto 2 fold but it increased to 50 fold when *cs* gene was expressed from its own promoter (Walsh and Koshland, 1985a). Thus it appears that CS activity in *E. coli* is controlled at the expression as well as protein level by complex processes which are not very clear.

Enhanced CS activity in *Pf* (pAB7) reduced the glucose consumption without affecting the specific growth and total glucose utilization rates and biomass yield which suggested the functioning of a feedback mechanism controlling the glucose influx. This effect on glucose utilization was contrary to the results of moderate overexpression (~2 fold) of CS in *E. coli* which showed no effect on glucose utilization while reduced glucose consumption rate by 50% when overexpressed upto 50 fold (Walsh and Koshland, 1985a). Additionally, reduced glucose consumption in *Pf* (pAB7) was counteracted by increased periplasmic glucose oxidation to gluconate as indicated by increase in gluconic acid levels and yields and corresponding GDH activity, maintaining the total glucose utilization similar to that in the control. These observations could not be correlated with *E. coli*, as it does not possess a functional direct oxidation pathway (van Shie et al., 1985). Unaltered biomass yield due to increase in CS activity was contradictory to the results in *E. coli* in which *glt*A overexpression increased the dry cell weight under aerobic conditions as mentioned earlier (De Maeseneire et al., 2006).

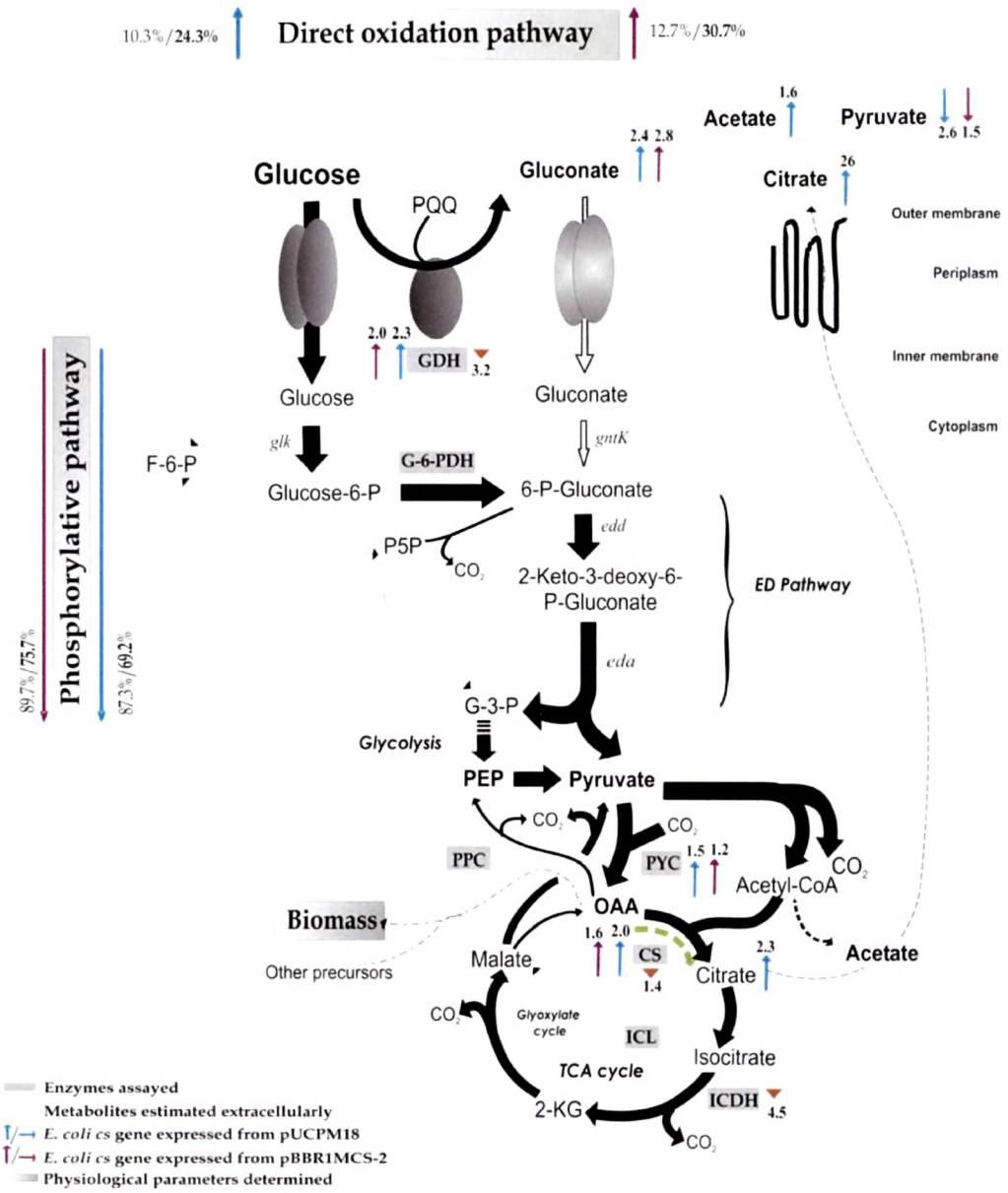

Fig. 5.7: Summarized effects of *E. coli cs* gene overexpression on glucose catabolism in *P. fluorescens* 13525. Numbers depicted over the arrows represent the fold change in response to *cs* overexpression on M9 minimal media with 100mM glucose. Numbers on the arrow heads (Δ) depict the fold variations between *Pf* (pAB8) and *Pf* (pBBR1MCS-2). Unchanged parameters are not indicated. The %values against the pink and the blue arrows represent the percentile glucose (calculated out of the total glucose utilized) distributed in phosphorylative and direct oxidation pathways in *Pf* (pAB8)/***Pf* (pAB7)** and *Pf* (pBBR1MCS-2)/***Pf* (pAB9)**. Details are discussed in the text.

Remarkably, extracellular citric acid levels and yields increased significantly by ~15 and 26 fold respectively which was accompanied by ~2 fold elevated intracellular citrate levels as a consequence of ~2 fold increase in CS activity. Accumulation of intracellular citric acid in *Pf* (pAB7) was similar to that of *E. coli* K and B *icd* mutants in which citrate accumulation was accompanied by ~3.8 and 2.5 fold increase in CS activity (Aoshima et al., 2003; Kabir and Shimizu, 2004). Unlike *E. coli icd* mutants, citrate accumulation in *Pf* (pAB7) had no negative effects on growth. Significant rise in extracellular citric acid levels in *Pf* (pAB7) is consistent with the presence of inherent citrate transporter. However, citric acid secretion by *E. coli* BL21(DE3) *icd* mutant on 2YT medium is unexplainable as it lacks citrate transporter (van der Rest et al., 1992; Aoshima et al., 2003). Considering the intracellular citrate levels, the extracellular levels detected in *Pf* (pAB7) were relatively low; which could be attributed to inefficient efflux transport of citrate. The active transport system for citrate excretion appears to be the main rate-determining factor in citrate overproduction by yeasts (Anastassiadis and Rehm, 2005) while in addition to citrate export, transport of sugar and ammonia into the cell are also crucial for citric acid production by *A. niger* (Papagianni, 2007).

Apart from the increased gluconic acid levels and yields as discussed earlier, concomitant reduction in pyruvic acid levels could be explained by increased PYC activity in *Pf* (pAB7), which could probably divert pyruvate flux towards increased OAA biosynthesis to meet the increased CS activity. Even in *A. niger* the enhancement of anaplerotic reactions replenishing TCA cycle intermediates predisposes the cells to form high amounts of citric acid (Legisa and Mattey, 2007). However, CS overproduction in *A. niger* did not affect PYC activity (Ruijter et al., 2000). Enhancement of biosynthetic reactions due to shortage of TCA cycle intermediates was also observed in citric acid accumulating *E. coli* K and B strains in the form of increased glyoxylate pathway (Aoshima et al., 2003; Kabir and Shimizu, 2004). However, similar increase in flux through glyoxylate shunt was not apparent in *Pf* (pAB7) as evident from very low and unaltered ICL activity detected in *Pf* (pAB8) and *Pf* (pAB7). Low ICL activity was consistent with earlier reports in *P. indigofera* in which ICL contributed negligibly to glucose metabolism (Howes and McFadden, 1962; Diaz-Perez et al., 2007).

In this context, increased PYC activity would increase the demand for CO_2 which although being important as second substrate of PYC is often neglected and can be

availed by from pyruvate transformation to acetyl-CoA (Alvarez-Vasquez et al., 2000; Papagianni, 2007). The stoichiometric requirement of the substrates by enhanced PYC reaction might increase the acetyl-CoA generating reaction which is probably reflected as increased acetate secretion by *Pf* (pAB7). The quantity of CO_2 released during acetyl-CoA formation in *A. niger* has been shown to be proportional to that utilized for OAA formation (Alvarez-Vasquez et al., 2000; Papagianni, 2007). This is also supported by increase in pyruvate dehdrogenase (acetyl-CoA generating) activity during optimal citrate production in *A. niger*.

Increase in CS activity in *Pf* (pAB9) by ~1.6 fold had similar effects on GDH and PYC activities and the physiological parameters to those in *Pf* (pAB7), albeit with significant quantitative differences (**Table 5.2; Fig. 5.5; 5.6**). Despite these similarities, citric acid was not detected in the extracellular medium of *Pf* (pAB9). This could be probably attributed to overall low metabolic rate as indicated by lower specific growth rate, and glucose utilization rates of *Pf* (pBBR1MCS-2) as compared to *Pf* (pAB8) (**Table 5.2**). These results are supported by significantly lower GDH, ICDH and CS activities in *Pf* (pBBR1MCS-2) as compared to *Pf* (pAB8). Hence, the intracellular citrate levels might be too low to get secreted and increase in CS activity further could not make any difference, thereby explaining absence of citrate in the extracellular medium of (pBBR1MCS-2) and *Pf* (pAB9). These metabolic differences may also be due to the differences in the copy numbers of pBBR1MCS-2 and pUCPM18 plasmids in *P. fluorescens* 13525, the former having higher plasmid copy number. Plasmid nature and copy number are known to exert load on cellular physiology leading to significant alterations in the metabolism (Neubauer et al, 2002; Wang et al., 2006; De Gelder, 2007).

In conclusion, CS appears to be "bottle-neck" enzyme in glucose metabolism of *P. fluorescens*. This study demonstrates a direct correlation of CS activity with citrate production which is contrary to earlier reports from the known citric acid producing microorganisms in which increased CS activity alone did not increase citric acid production. *E. coli* required a TCA block in the form of *icd* mutation leading to increased CS activity and enhanced anaplerotic reactions; *A. niger* was predicted to require ~13 different enzyme manipulations including elevated CS activity; while in plants it appears to be due to Al toxicity rather than *cs* overexpression (de la Fuente et al., 1997; Alvarez-

Vasquez et al., 2000; López-Bucio et al., 2000; Ruijter et al., 2000; Delhaize et al., 2001; Guebel and Torres Darias, 2001). Increasing CS activity in *P. fluorescens* for citric acid overproduction from glucose could be a better strategy than *icd* mutation in *E. coli* as the former overcomes the limitations of reduced biomass and absence of citrate secreting mechanism in the latter. These results highlight one of the crucial aspects of metabolic engineering that the desired and predicted outcomes of targeted genetic manipulation not only depend on the choice of targeted modification but also largely depend on the host metabolic regulatory circuit.